Organically Templated Mixed-Valent Iron Sulfates Possessing Kagomé and Other Types of Layered Networks

Geo Paul, Amitava Choudhury,
E. V. Sampathkumaran, and C. N. R. Rao*

We have been interested in developing strategies for designing new open-framework architectures. One such strategy is the case of the sulfate tetrahedron and its utilization as a primary building unit, in place of the silicate or the phosphate tetrahedron commonly employed for the purpose.[1,2] Our efforts in this direction have enabled us to obtain organically templated open-framework metal sulfates under hydrothermal conditions with one-dimensional chain structures as well as two-dimensional layered structures.[3] In the case of iron sulfates, Fe is present generally in the $+2$ or the $+3$ oxidation state; they all show the presence of antiferromagnetic interactions. In this communication, we report the successful synthesis of organically templated mixed-valent iron sulfates of the compositions, $[H_2N(CH_2)_4NH_2]_2[Fe^{III}_2Fe^{II}_3F_{12}(SO_4)_2(H_2O)_2]$ (**1**) and $[HN(CH_2)_6NH][Fe^{III}Fe^{II}_2F_6(SO_4)_2]\cdot[H_3O]$ (**2**), with novel structural features and magnetic properties. In particular, **2** is an unusual example of an iron compound with a perfect Kagomé structure. The discovery of such an unusual Kagomé lattice is significant considering the current interest in these compounds[4] and the fact that iron compounds possessing the Kagomé lattice generally contain Fe in a single oxidation state.

The asymmetric unit of **1** contains four crystallographically distinct iron atoms and one sulfur atom. The fluorine and oxygen neighbors are coordinated octahedrally to the Fe atoms ($Fe(1)F_5O$, $Fe(2)F_4O_2$, $Fe(3)F_2O_2(H_2O)_2$ and $Fe(4)F_4O_2$). The structure of **1** is constructed from the anionic framework layers of $[Fe^{III}_2Fe^{II}_3F_{12}(SO_4)_2(H_2O)_2]^{4-}$. The $Fe(2)F_4O_2$ and $Fe(4)F_4O_2$ octahedra are vertex-shared through *trans*-Fe-F-Fe linkages to form an infinite chain along the *a* axis. Such chains are connected by an edge-shared trimer of two $Fe(1)F_5O$ and one $Fe(3)F_2O_4$ octahedra to yield a layered network in the *ac* plane. In the trimer, the $Fe(3)F_2O_4$ octahedra are flanked by two $Fe(1)F_5O$ octahedra. Such connectivity creates a triangular lattice formed by $Fe(1)F_5O$, $Fe(2)F_4O_2$, and $Fe(4)F_4O_2$ octahedra. The SO_4 tetrahedron caps the triangular lattice, creating a 10-membered aperture within the layer, as shown in Figure 1a. The layers are stacked one over the other along the *b* axis in *AAAA* fashion and are held together by hydrogen bonding interactions with the diprotonated piperazine (PIP) molecules residing in the interlamellar space (see Figure 1b). The bond lengths and

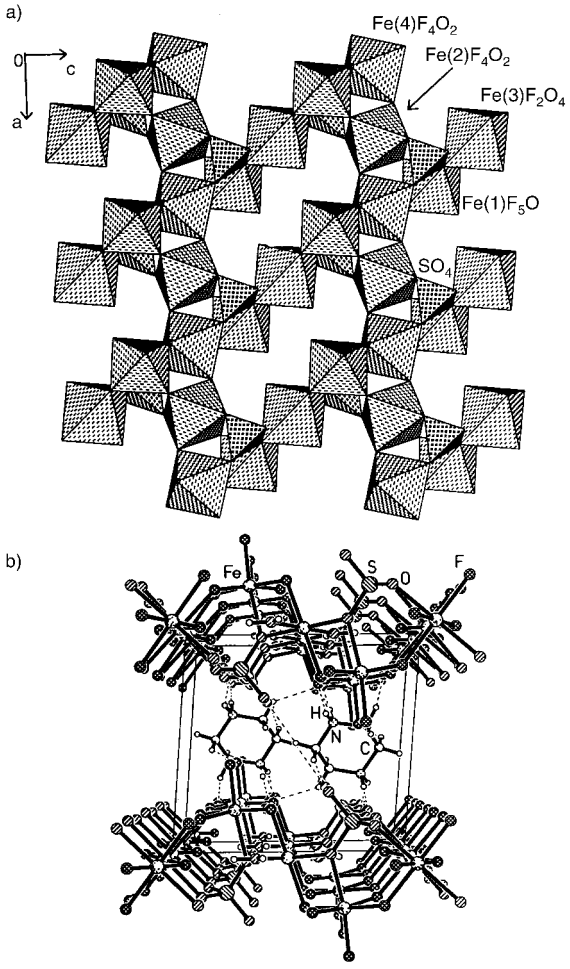

Figure 1. a) Polyhedral view of the $[Fe^{III}_2Fe^{II}_3F_{12}(SO_4)_2(H_2O)_2]^{4-}$ layer in **1**, viewed perpendicular to the *ac* plane. Here, Fe(1) is in the $+3$ oxidation state and the remaining iron atoms are in the $+2$ state. Note the symmetrical capping of the sulfate tetrahedra in the triangular lattice and the 10-membered aperture within the layer; b) Structure of **1** showing the presence of the amine group located in the interlayer space.

angles indicate perfect octahedral geometry around Fe^{II}-centers and a slightly distorted geometry for the Fe^{III} centers. Bond-valence sum (BVS) calculations[5] ($Fe(1) = 3.03$, $Fe(2) = 2.02$, $Fe(3) = 1.98$, and $Fe(4) = 2.05$) and the average Fe–O/F bond lengths indicate the oxidation state of Fe(1) to be $+3$, and the remaining Fe centers to be $+2$. The positions of the fluorine atoms find indirect support from BVS calculations ($F(1) = 0.616$, $F(2) = 0.563$, $F(3) = 0.896$, $F(4) = 0.804$, $F(5) = 0.786$ and $F(6) = 0.74$). The mixed-valent nature of **1** was also confirmed by Mössbauer spectroscopy. DC magnetic susceptibility data (at 100 Oe) show a sharp magnetic transition around 15 K and what appears to be a ferrimagnetic transition at around 3 K, the field-cooled (FC) and the zero-field-cooled (ZFC) data being identical (Figure 2a). The inverse susceptibility data recorded at 5 kOe (Figure 2b) show a linear

[*] Prof. Dr. C. N. R. Rao, G. Paul, A. Choudhury
Chemistry and Physics of Materials Unit and
CSIR Center of Excellence in Chemistry
Jawaharlal Nehru Center for Advanced Scientific Research
Jakkur, P.O., Bangalore 560 064 (India)
Fax: (+91) 80-846-2766
E-mail: cnrrao@jncasr.ac.in
Prof. Dr. C. N. R. Rao, A. Choudhury
Solid State and Structural Chemistry Unit
Indian Institute of Science
Bangalore 560 012 (India)
Prof. Dr. E. V. Sampathkumaran
Department of Condensed Matter Physics and Materials Science
Tata Institute of Fundamental Research
Mumbai 400005 (India)

  0044-8249/02/4122-4297 $ 20.00+.50/0

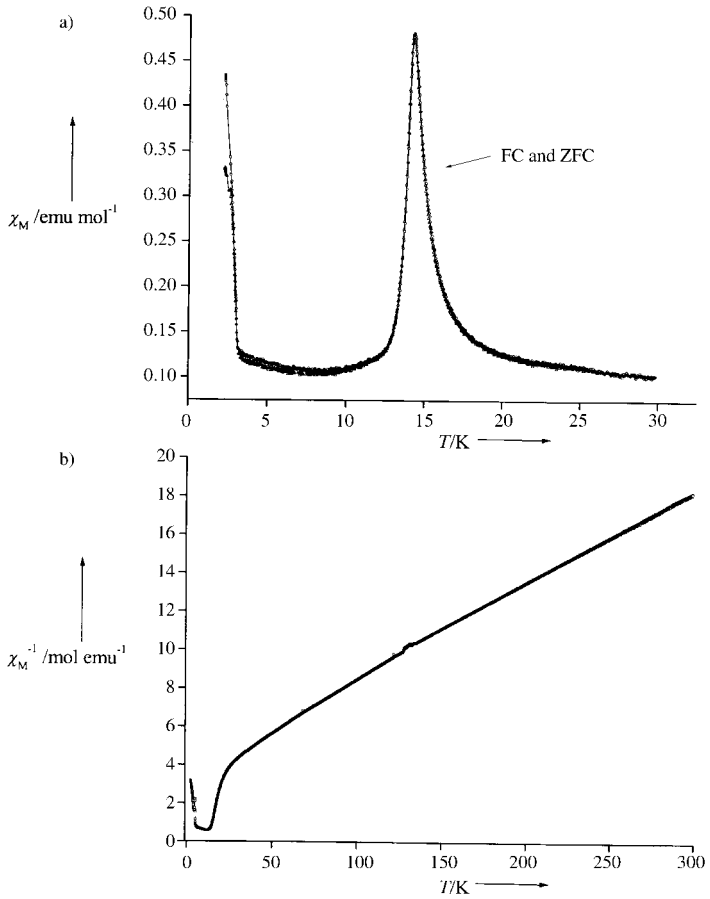

Figure 2. a) Temperature dependence of the DC magnetic susceptibility of **1** measured at 100 Oe under field-cooled (FC) and zero-field-cooled (ZFC) conditions; b) Temperature variation of the inverse DC susceptibility measured at 5 kOe.

behavior at high temperatures, which yields a negative Curie temperature ($T_c = -86$ K). These data also reveal a transition to a canted antiferromagnetic state at low temperatures.

The asymmetric unit of **2** contains 28 non-hydrogen atoms, of which 21 belong to the inorganic framework and seven belong to the extra-framework guest molecules; one extra-framework oxygen atom belongs to the hydronium ion. The structure of **2** consists of anionic layers of vertex-sharing $Fe^{III}F_4O_2$ and $Fe^{II}F_4O_2$ octahedra and tetrahedral SO_4 units, which are fused together by $Fe^{III/II}$-F-$Fe^{III/II}$ and $Fe^{III/II}$-O-S moieties. Each $Fe^{III/II}F_4O_2$ unit shares four of its $Fe^{III/II}$–F vertices with similar neighbors, with the $Fe^{III/II}$-F-$Fe^{III/II}$ bonds roughly aligned in the *ab* plane. The $Fe^{III/II}$–O bond is canted from the *ab* plane and this $Fe^{III/II}$–O vertex effectively forces a three-ring trio of apical $Fe^{III/II}$–O bonds closer together to allow them to be capped by the SO_4 tetrahedra. The three- and six-rings of octahedra result from the in-plane connectivity, as shown in Figure 3a. The layers in **2** are typical of a Kagomé lattice with hexagonal tungsten bronze-type sheets [6] of vertex-sharing $Fe^{III/II}F_4O_2$ octahedra, as shown in Figure 3b. The amine molecules are present between the layers just as in **1**. The structure of **2** is akin to that of the mineral jarosite[7] where all of the Fe atoms are in the +3 oxidation state. The Fe–O bond lengths in **2** are in the range 2.003(3)–2.149(3) Å ($(Fe(1)–O)_{av}$ 2.140(3), $(Fe(2)–O)_{av}$ 2.146(3), and $(Fe(3)–O)_{av}$ 2.011(3) Å), and the Fe–F bond lengths are in the range 1.906(2)–2.157(2) Å ($(Fe(1)–F)_{av}$ 2.081(2), $(Fe(2)–F)_{av}$ 2.080(2), and $(Fe(3)–F)_{av}$ 1.936(2) Å). BVS calculations (Fe(1) = 1.93, Fe(2) = 1.92, and Fe(3) = 3.01) as well as the average bond distances indicate that the oxidation state of Fe(1) and Fe(2) is +2 and that of Fe(3) is +3. The positions of the six F atoms are also supported by the bond valence calculations (F(1) = 0.734, F(2) = 0.669, F(3) = 0.797, F(4) = 0.70, F(5) = 0.76, and F(6) = 0.71). Thus, the framework stoichiometry of the $[Fe^{III}Fe^{II}_2F_6(SO_4)_2]$ unit with a −3 charge requires the amine to be doubly protonated, in addition to the presence of the hydronium ion. Mössbauer spectra also confirm the presence of the Fe^{II} and Fe^{III} states in the ratio 2:1.

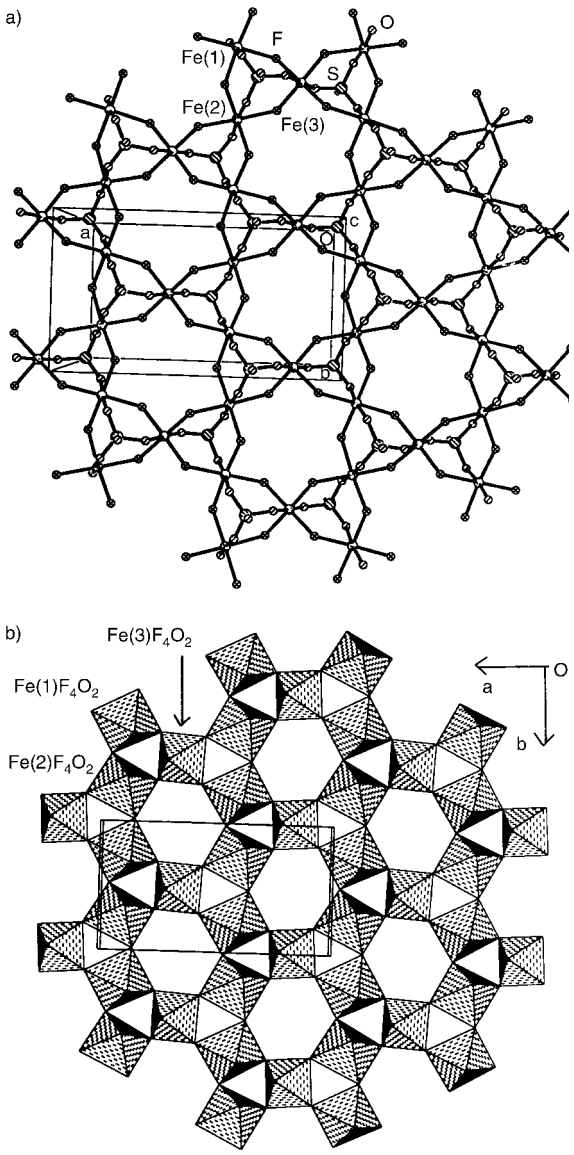

Figure 3. a) Ball-and-stick representation of a section of $[Fe^{III}Fe^{II}_2F_6(SO_4)_2]^{3-}$ in **2**, which shows the presence of the 3- and 6-rings; the 3-rings are capped by the sulfate tetrahedra; b) Polyhedral view of the 2D network of corner-sharing iron octahedra in **2**, viewed perpendicular to the *ab* plane. Here, Fe(1) and Fe(2) are in the +2 oxidation state and Fe(3) is in the +3 state.

The Kagomé lattice in **2** is unusual in several respects. There is 100% occupation of the iron sites[8] and this is the first

  0044-8249/02/4122-4298 $ 20.00+.50/0

example of a Kagomé lattice where the Fe centers are found in two oxidation states. Extensive protonation of the OH sites in jarosite results in vacancies in the Fe lattice, but we seem to be able to overcome this problem by replacing OH groups with fluorine atoms. The magnetic behavior of **2** is quite different from that of **1** and is even more complex. Compound **2** shows magnetic frustration, as typified by the divergence in the FC and ZFC magnetization data shown in Figure 4a. The spin-freezing temperature (T_f) is around 12 K.[9] AC susceptibility measurements confirm a typical spin-glass transition behavior. The inverse magnetic susceptibility data recorded at 5 kOe are linear at high temperatures giving a negative Curie temperature ($T_c = -180$ K). The data show a ferrimagnetic-type transition, as can be seen from Figure 4b. This unusual behavior of **2** requires further study. It may be noted that most of the Fe compounds with the Kagomé lattice show either spin-glass behavior or long-range antiferromagnetic ordering.[4,10,11] The only other Kagomé-type structures exhibiting ferromagnetic features are the vanadium compound reported by Grohol et al.[12] and the dimeric copper compound reported by Zaworotko and co-workers[13] The magnetic moment obtained by extrapolating the high-field [12 T] portion of M versus H to $H = 0$ is 2.95 μ_B mol^{-1} at 10 K for **2** (calcd 9 μ_B mol^{-1}), compared to 4.8 μ_B mol^{-1} for **1** (calcd 16 μ_B mol^{-1}). It should be noted that other mixed-valent iron compounds comparable to **2** exhibit entirely different magnetic properties. Thus $[Fe_3F_8(H_2O)_2]$, with hexagonal bronze-type layers, is antiferromagnetic (Néel temperature, $T_N = 157$ K) and shows weak ferromagnetism at low temperatures.[14] $[Fe_2F_5(H_2O)_2]$, with an inverse weberite structure, is ferrimagnetic ($T_C = 48$ K).[15] Na_2NiFeF_7, with the weberite structure, is also ferrimagnetic ($T_C = 88$ K)[16] while in $BaMnFeF_7$, ferromagnetic sublattices of Mn and Fe are coupled antiferromagnetically giving a T_N value of 85 K.[17] In contrast, compound **2** exhibits a clear spin-glass behavior, as well as ferrimagnetism.

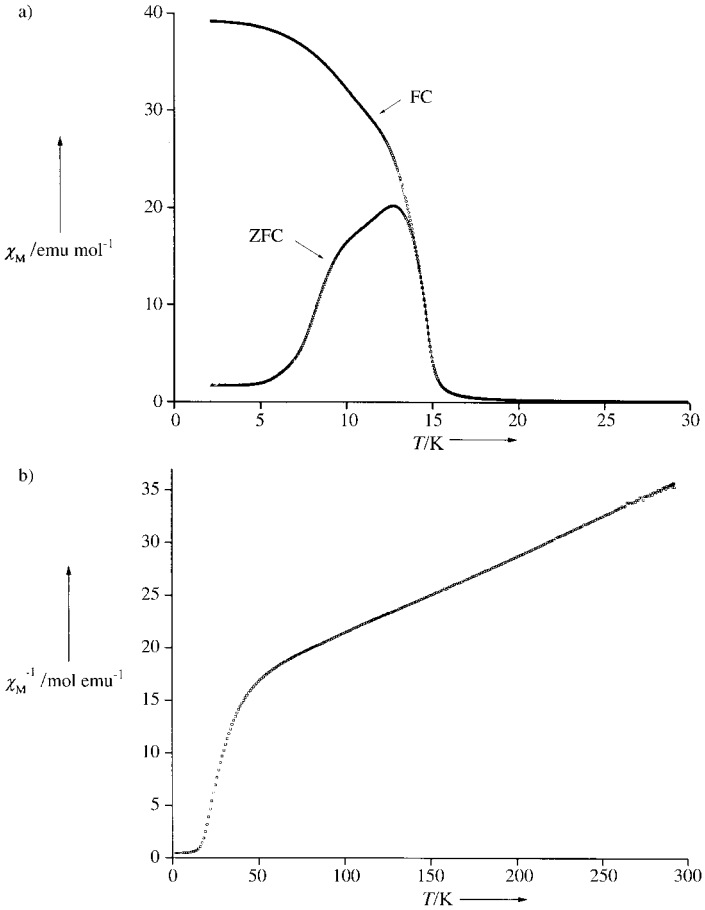

Figure 4. a) DC susceptibility data of **2** measured at 100 Oe which displays the divergence between the ZFC and FC measurements; b) Temperature variation of the inverse DC susceptibility measured at 5 kOe.

Besides demonstrating that the sulfate tetrahedron can be conveniently employed to generate novel organically templated transition metal sulfates, the present study reveals that layered mixed-valent iron sulfates have unusual magnetic properties. The mixed-valent iron Kagomé compound deserves to be further explored both experimentally and theoretically.

Experimental Section

The synthesis of **1** and **2** was carried out in teflon-lined acid digestion bombs with an internal volume of 23 cm^3 under constant pressure by heating the starting mixture at 180 °C for 2 days. Compound **1** was prepared from the following reagents: ferric citrate (1 mmol), piperazine sulfate[18] (4 mmol), HF (48%, 8 mmol), H_2O (50 mmol), and ethylene glycol (50 mmol). The product (yield 50%), which consisted of red rod-shaped crystals, was monophasic. Compound **2** was prepared from the following reagents: ferric citrate (1 mmol), H_2SO_4 (98%, 4 mmol), 1,4-diazabicyclo[222]octane (DABCO, 6 mmol), HF (48%, 4 mmol), H_2O (50 mmol), and *n*-butanol (30 mmol). The product (yield = 40%), consisting of red hexagonal plate-shaped crystals was monophasic. The identities of **1** and **2** were established by various techniques, which included X-ray crystallography. X-ray powder diffraction patterns of **1** and **2** were in good agreement with the simulated patterns based on single-crystal data, indicative of their phase purity. The Fe:S ratios in **1** and **2** were determined by energy-dispersive X-ray analysis (EDAX) to be 5:2 and 3:2, respectively, which is commensurate with their molecular formulas. Furthermore, thermogravimetric analysis gave the exact mass losses expected for the removal of water, amine, and SO_3 in both **1** and **2**. The final product of the decomposition of **1** was Fe_2O_3, which was also verified from its powder XRD pattern. Complex **2** gave FeO as the final product. The fluorine analysis was also satisfactory, which indicated that the OH groups are, generally, replaced by fluorine atoms.

Structure determination: Single-crystal data were collected on a Siemens SMART-CCD diffractometer (graphite-monochromated $Mo_{K\alpha}$ radiation, $\lambda = 0.71073$ Å, $T = 298$ K). An absorption correction based on symmetry-equivalent reflections was applied using SADABS.[19] The structures were solved by direct methods using SHELXS-86[20] and difference Fourier synthesis. Full-matrix least-squares structure refinement against $|F^2|$ was carried out using the SHELXTL-PLUS[21] package of programs. Hydrogen positions for the bonded water molecule (O(3) in **1**) as well as the extra-framework hydronium ion (O(100) in **2**) were located from the difference Fourier map and placed in the observed position and refined isotropically. All the remaining hydrogen positions for **1** and **2** were initially located in the difference Fourier maps, and for the final refinement, the hydrogen atoms were placed geometrically and held in the riding mode. The non-hydrogen atoms were refined anisotropically.

Crystal data. **1**: $M_r = 911.72$, triclinic, space group = $P\bar{1}$ (no. 2), $a = 7.222(2)$, $b = 9.043(2)$, $c = 9.463(4)$ Å, $\alpha = 94.58(3)$, $\beta = 91.71(2)$, $\gamma = 95.08(2)$°, $V = 613.2(3)$ Å^3, $Z = 2$, $\mu = 3.204$ mm^{-1}, $\rho_{calcd} = 2.469$ mg m^{-3}, 1724 unique reflections ($R_{int} = 0.0208$), final $R = 0.0359$, $R_W = 0.0905$, GOF = 1.043. **2**: $M_r = 606.89$, orthorhombic, space group = $Pna2_1$ (no. 33), $a = 12.9269(6)$, $b = 7.4091(3)$, $c = 17.5970(8)$ Å, $\alpha = \beta = \gamma = 90$°, $V = 1685.38(13)$ Å^3, $Z = 4$, $\mu = 2.908$ mm^{-1}, $\rho_{calcd} = 2.392$ mg m^{-3}, 2362 unique reflections ($R_{int} = 0.0333$), final $R = 0.0243$, $R_w = 0.0562$, GOF = 1.000.

  0044-8249/02/4122-4299 $ 20.00+.50/0

CCDC-185168 (**1**) and CCDC-185167 (**2**) contains the supplementary crystallographic data for this paper. These data can be obtained free of charge via www.ccdc.cam.ac.uk/conts/retrieving.html (or from the Cambridge Crystallographic Data Centre, 12, Union Road, Cambridge CB21EZ, UK; fax: (+44) 1223-336-033; or deposit@ccdc.cam.ac.uk).

Received: May 14, 2002
Revised: August 26, 2002 [Z19300]

[1] a) D. W. Breck, *Zeolite Molecular Sieves*, Wiley, New York, **1974**; b) W. M. Meier, D. H. Oslen, C. Baerlocher, *Atlas of Zeolite Structure Types*, Elsevier, London, **1996**.
[2] A. K. Cheetham, G. Férey, T. Loiseau, *Angew. Chem.* **1999**, *111*, 3466 – 3492; *Angew. Chem. Int. Ed.* **1999**, *38*, 3268 – 3292.
[3] a) A. Choudhury, J. Krishnamoorthy, C. N. R. Rao, *Chem. Commun.* **2001**, 2610 – 2611; b) G. Paul, A. Choudhury, C. N. R. Rao, *Chem. Commun.* **2002**, 1904 – 1905.
[4] a) A. P. Ramirez, *Annu. Rev. Mater. Sci.* **1994**, *24*, 453 – 480; b) J. E. Greedan, *J. Mater. Chem.* **2001**, *11*, 37 – 53; c) A. S. Wills, A. Harrison, *J. Chem. Soc. Faraday Trans.* **1996**, *92*, 2161 – 2166; d) T. Inami, M. Nishiyama, S. Maegawa, Y. Oka, *Phys. Rev. B* **2000**, *61*, 12181 – 12186; e) J. N. Reimers, A. J. Berlinsky, *Phys. Rev. B* **1993**, *48*, 9539 – 9554; f) J. Frunzke, T. Hansen, A. Harrison, J. S. Lord, G. S. Oakley, D. Visser, A. S. Wills, *J. Mater. Chem.* **2001**, *11*, 179 – 185.
[5] a) N. E. Brese, M. O'Keeffe, *Acta Crystallogr. Sect. B* **1991**, *47*, 192 – 197; b) I. D. Brown, D. Altermatt, *Acta Crystallogr. Sect. B* **1985**, *41*, 244 – 247.
[6] A. Magneli, *Acta Chem. Scand.* **1953**, *7*, 315.
[7] a) J. E. Dutrizac, S. Kaiman, *Can. Mineral.* **1976**, *14*, 151 – 158; b) F. C. Hawthrone, S. V. Krivovichev, P. C. Burns, *Rev. Mineral. Geochem.* **2000**, *40*, 1 – 101.
[8] A. S. Wills, A. Harrison, S. A. M. Mentink, T. E. Mason, Z. Tun, *Europhys. Lett.* **1998**, *42*, 325 – 330.
[9] a) G. S. Oakley, D. Visser, J. Frunzke, K. H. Andersen, A. S. Wills, A. Harrison, *Phys. B* **1999**, *267–268*, 142 – 144; b) A. Harrison, A. S. Wills, C. Ritter, *Phys. B* **1998**, *241–243*, 722 – 723.
[10] H. Serrano-Gonzalez, S. T. Bramwell, K. D. M. Harris, B. M. Kariuki, L. Nixon, I. P. Parkin, C. Ritter, *Phys. Rev. B* **1999**, *59*, 14451 – 14460.
[11] a) G. S. Oakley, S. Pouget, A. Harrison, J. Frunzke, D. Visser, *Phys. B* **1999**, *267–268*, 145 – 148; b) A. S. Wills, A. Harrison, C. Ritter, R. I. Smith, *Phys. Rev. B* **2000**, *61*, 6156 – 6169; c) E. A. Earle, A. P. Ramirez, R. J. Cava, *Phys. B* **1999**, *262*, 199 – 204; d) S.-H. Lee, C. Broholm, M. F. Collins, L. Heller, A. P. Ramirez, Ch. Kloc, E. Bucher, R. W. Erwin, N. Lacevic, *Phys. Rev. B* **1997**, *56*, 8091 – 8097.
[12] a) D. Grohol, D. Papoutsakis, D. G. Nocera, *Angew. Chem.* **2001**, *113*, 1567 – 1569; *Angew. Chem. Int. Ed.* **2001**, *40*, 1519 – 1521; b) D. Papoutsakis, D. Grohol, D. G. Nocera, *J. Am. Chem. Soc.* **2002**, *124*, 2647 – 2656; c) D. Grohol, D. G. Nocera, *J. Am. Chem. Soc.* **2002**, *124*, 2640 – 2646.
[13] B. Moulton, J. Lu, R. Hajndl, S. Hariharan, M. J. Zaworotko, *Angew. Chem.* **2002**, *114*, 2945 – 2948; *Angew. Chem. Int. Ed.* **2002**, *41*, 2821 – 2824.
[14] a) M. Leblanc, G. Férey, Y. Calage, R. De Pape, *J. Solid State Chem.* **1984**, *53*, 360 – 368; b) M. Leblanc, G. Férey, P. Lacone, J. Punnetier, *J. Magn. Magn. Mater.* **1991**, *92*, 359 – 365.
[15] Y. Laligant, M. Leblanc, J. Pannetier, G. Férey, *J. Phys. C* **1986**, *19*, 1081 – 1095.
[16] Y. Laligant, Y. Calage, G. Heger, J. Pannetier, G. Férey, *J. Solid State Chem.* **1989**, *78*, 66 – 77.
[17] P. Lacorre, J. Pannetier, J. Pebler, S. Nagel, D. Babel, A. De Kozak, M. Samouel, G. Férey, *J. Solid State Chem.* **1992**, *101*, 296 – 308.
[18] K. Jayaraman, A. Choudhury, C. N. R. Rao, *Solid State Sci.* **2002**, *4*, 413 – 422.
[19] G. M. Sheldrick, SADABS Siemens Area Detector Absorption Correction Program, University of Göttingen, Göttingen (Germany), **1994**.
[20] a) G. M. Sheldrick, SHELXS-86 Program for crystal structure determination, University of Göttingen, **1986**; b) G. M. Sheldrick, *Acta Crystallogr. Sect. A* **1990**, *35*, 467.
[21] G. M. Sheldrick, SHELXTL-PLUS Program for Crystal Structure Solution and Refinement, University of Göttingen, Göttingen (Germany).

Ionic Liquids Containing Anionic Selenium Species: Applications for the Oxidative Carbonylation of Aniline**

Hoon Sik Kim,* Yong Jin Kim, Hyunjoo Lee, Kun You Park, Chongmok Lee, and Chong Shik Chin

Non-phosgene processes for the synthesis of carbamates and/or substituted ureas have attracted increasing interest in recent years, particularly in the area of green chemistry because of the environmental concern regarding the use of highly toxic phosgene.[1] Of the various non-phosgene processes, one approach involves the catalytic oxidative carbonylation of an amine in the presence of an appropriate catalyst or catalytic system.[2]

In previous reports, we have demonstrated that alkali metal-containing selenium compounds, obtained from the reaction of SeO_2 and M_2CO_3 (M = alkali metal) in methanol, are effective catalysts for the oxidative carbonylation of aniline to produce phenyl carbamate and diphenylurea.[3] The major disadvantage of using these selenium compounds is the difficulty in separating the product and the catalyst from the reaction mixture, which arises from the coproduction of insoluble diphenylurea and soluble alkyl phenyl carbamate, with high conversion of aniline. A further disadvantage is the formation of small quantities of unknown, highly volatile, malodorous, and possibly toxic selenium species at relatively high reaction temperatures.

Recently, there have been a considerable number of papers regarding ionic liquids and their use in immobilizing volatile, precious, and/or toxic homogeneous catalysts, thereby improving the stability and facilitating the recovery of the catalyst.[4]

In this context, the alkali metal-containing selenium compound $[KSeO_2(OCH_3)]$ can be reacted with 1-alkyl-3-methylimidazolium chlorides to prepare new imidazolium-based ionic liquids containing anionic selenium species. The ionic liquids are found to show surprisingly high activity for the

[*] Dr. H. S. Kim
CFC Alternatives Research Center
KIST
39-1, Hawolgokdong, Seongbukgu, Seoul 136-791 (Korea)
Fax: (+82) 2-958-5859
E-mail: khs@kist.re.kr
H. Lee, K. Y. Park
Korea Institute of Science and Technology
Seoul (Korea)
Prof. C. Lee
Department of Chemistry
Ewha Womans University
Seoul (Korea)
Y. J. Kim, Prof. C. S. Chin
Department of Chemistry
Sogang University
Seoul (Korea)

[**] This work was supported by the Ministry of Science and Technology. We thank to Prof. Myoung Soo Lah for the X-ray crystallographic analysis at Hanyang University.

Supporting information for this article is available on the WWW under http://www.angewandte.org or from the author.

